Coastal acid sulfate soil processes in Barker Inlet, South Australia

Doctor of Philosophy

The University of Adelaide

School of Earth and Environmental Sciences

Brett P. Thomas

September 2010

Chapter Ten

10. Mineralogy: storage of trace elements in sulfate-rich salt efflorescences and iron sulfides

Salt efflorescences in acid sulfate soil environments can form on the banks of drains, creek depressions, mud flats and spoil heaps by capillary migration and evaporation of hypersaline groundwaters and pore waters during dry seasons. Salt efflorescences are a product of mineral weathering and groundwater in acid sulfate soil environments. The formation and transformation of salt efflorescences can control the geochemistry of acid sulfate waters, which in turn, influences the behaviour of trace elements and drainage water quality. Under acidic conditions (pH < 4), precipitation of hydroxysulfates and oxyhydroxides of Fe and Al may scavenge potentially toxic elements such as As, Cd, Cu, Pb, V and Zn (Jambor and Blowes 1994; Keith *et al.* 2001; Nordstrom and Alpers 1999). Because salt efflorescences can have high solubilities in water, they have a potential to impact drainage water quality when they dissolve following rain events.

The main purpose of this chapter is to: **(i)** provide a brief review of the major Fe minerals, Al minerals and sulfate-rich salts occurring in acid sulfate soils, **(ii)** report on mineralogical analyses, using X-ray diffraction (XRD) and scanning electron microscopy (SEM), of salt efflorescence and sulfide samples and evaluate their potential to store trace elements, **(iii)** construct descriptive and predictive soil-regolith toposequence process models to explain seasonal mineral formation and transformation processes, and **(iv)** evaluate the impact of excavating drains in existing coastal acid sulfate soils containing sulfuric material at the Gillman study site. This was done by excavating a new, 100 m long, 1.8 m deep experimental drain through acid sulfate soils at Gillman Focus area A and monitoring changes in mineral formation-transformation along the open drain walls and seasonal changes in drainage water quality.

Motivation for this study was compounded when land managers for the Gillman area proposed to re-direct a major stormwater drain through the centre of the Gillman study

site (requiring excavations through map units 5 and 6), which comprise acid sulfate soils containing sulfuric and hypersulfidic materials.

10.1. Introduction

The excavation of drains can cause extreme changes in hydrology and geochemistry in acid sulfate soil landscapes and many iron and sulfate minerals are likely to form or transform rapidly when exposed to air. Iron minerals, especially in the form of oxyhydroxides, hydroxides and oxides, are ubiquitous in almost all oxidised acid sulfate soil environments (Figure 10-1). In acid sulfate soils, Fe plays a fundamental role in many biologically mediated processes (Berner 1984). Bacterial activity is frequently involved in both the degradation and formation of Fe sulfide phases, and can be involved in all forms of secondary iron mineralisation from the transformation of Fe phases in natural mineral sites. The colour, form, crystallite size and concentration of substituted cations in iron minerals can be used quantitatively as indicators of such specific soil processes (e.g. Bigham *et al.* 2002; Schwertmann and Fitzpatrick 1992).

NOTE:
This figure is included on page 299 of the print copy of the thesis held in the University of Adelaide Library.

Figure 10-1 schematic diagram for the formation of pyrite in anoxic environments (after Berner 1984).

The excavation of drains in acid sulfate soils is known to cause: **(i)** rapid oxidation of (remaining) pyrite, and **(ii)** formation of a wide range of oxyhydroxysulfates, oxyhydroxides and sulfate- containing minerals within the soil profile and on the exposed sides of the drains (e.g. Bigham *et al.* 2002; Fitzpatrick 1988; Fitzpatrick *et al.* 1993a). The type and relative proportions of the secondary sulfate and iron minerals that may occur depends critically on the soil solution chemistry, in particular, Eh, pH and ionic concentrations. Depending on the specific environmental condition, the neo-formed secondary Fe minerals (and Al minerals) are predominantly oxides, oxyhydroxides, sulfides, sulfates, carbonates and phosphates. Figure 10-1 lists the commonly occurring sulfides, carbonates, salts, oxyhydroxides, hydroxides and oxide phases that occur in acid sulfate soils, together with respective mineralogical occurrence and distribution in soil environments, although it is by no means a comprehensive list of all the Fe phases that could be found in acid sulfate soil (Bigham *et al.* 2002; Fitzpatrick and Self 1997; Schwertmann and Fitzpatrick 1992).

Acidification of soils occurs if the amount of acidity produced exceeds the pH buffering capacity (the overall neutralizing capacity) of the soil. For sulfuric materials, the soluble products of the chemical reactions can: **(i)** remain as dissolved constituents of soil pore waters, **(ii)** form a range of secondary minerals in the form of efflorescences comprising sulfate-rich salts that accumulate due to evaporation (e.g. epsomite and hexahydrite), **(iii)** undergo a series of hydrolysis reactions and precipitate new minerals such as iron oxyhydroxides and iron oxyhydroxysulfates (e.g. jarosite, natrojarosite, schwertmannite and sideronatrite), and **(iv)** accelerate the weathering or dissolution of minerals in soils and sediments by removing reaction products. The hydroxysulfate minerals formed under acidic conditions are important to recognize because they store acidity and metals that can subsequently generate poor water quality if they are dissolved. Several studies have shown that dissolution of salt accumulations along stream banks during a rainstorm temporarily lowers pH and increases metal loads in streams (Fitzpatrick *et al.* 2009; Jerz and Rimstidt 2003). Such water quality impacts can have damaging effects on aquatic ecosystems and can complicate efforts to remediate acid drainage. Salt efflorescences may or may not be present at a given site on a given day, depending on weather conditions.

Table 10-1 summary of the occurrence and distribution of secondary Fe oxides, sulfides, carbonates and salts in soil environments (after Bigham *et al.* 2002; Fitzpatrick and Shand 2008).

Mineral	Dominant colour	Soil Environment	†Landscape position
Hematite [α-Fe_2O_3]	Red (< 0.5mm) Reddish-purple (>0.5mm nodules, mottles, ferricretes)	Aerobic soils of the tropics, subtropics, arid/semiarid zones; greater amounts with warmer temperatures and low organic matter content.	Well drained upper parts.
Goethite [α-FeO(OH)]	Yellow (< 0.5 mm). Strong brown (>0.5mm nodules, ferricretes)	All weathering regimes; greater amounts with cool, wet climates (including higher altitudes and moist/cool aspects) and elevated organic matter.	Well drained upper parts and mottles in mid-slopes.†
Lepidocrocite [γ-FeO(OH)]	Orange (<0.5mm) Reddish-purple (>0.5mm)	Seasonally anaerobic, non-calcareous soils of cool-temperate climates (including higher altitudes and moist/cool aspects on mid to lower slopes).	Seasonally wet mid-slopes.
Ferrihydrite [$5Fe_2O_3.9H_2O$]	Reddish-brown	Soils subject to rapid oxidation of Fe in the presence of organic matter.	Seasonally wet foot-slopes and seeps.
Maghemite [γ-Fe_2O_3]	Brown.	Highly weathered soils of the tropics and subtropics derived from mafic rocks rich in precursor magnetite and/or soils subjected to burning in the presence of organic matter.	Well drained upper parts and foot-slopes after burning.
Schwertmannite [$Fe_8O_8(OH)_{4.6}(SO_4)_{1.7}$]	Reddish-orange	Sulfuric material in acid sulfate soils of both coastal and inland areas; anthropogenic sites such as mines, spoils and tailings. pH between 3.5 and 4.5.	Poorly drained foot-slopes, seeps and bottom lands.
Jarosite [$KFe_3(SO_4)_2(OH)_6$] **Natrojarosite** [$NaFe_3(SO_4)_2(OH)_6$]	Pale yellow	Sulfuric material in acid sulfate soils of both coastal and inland areas; anthropogenic sites including mines, spoils and tailings. pH between 2.5 and 3.5.	Poorly drained foot-slopes, seeps and bottom lands.
***Sideronatrite** [$Na_2Fe(SO_4)_2.OH.3H_2O$]	Pale yellowish green	Sulfuric material in acid sulfate soils in inland or coastal back swamps; anthropogenic sites such as mines, spoils and tailings. pH between 2.0 and 3.5.	Poorly drained foot-slopes, seeps and bottom lands.
Fougerite [$(Fe^{2+}, Mg)_6 (Fe^{3+})_2 (OH)_{18}\bullet 4(H_2O)$]	Bluish-grey	Strongly hydromorphic soils.	Poorly drained foot-slopes, seeps and bottom lands.
Iron hydroxycarbonate (chukanovite) $Fe_2(OH)_2CO_3^{2-}$	Bluish-green	Strongly hydromorphic and subaqueous soils.	Poorly drained foot-slopes, seeps and bottom lands.
Akaganéite [β-FeOOH]	Bright Orange	Strongly hydromorphic and subaqueous soils.	As above and in saline rivers, lakes and ocean
Iron monosulfides [FeS]	Black	Strongly hydromorphic and subaqueous soils.	As above and in rivers and lakes.
Iron disulfides or pyrite [FeS_2]	Black	Strongly hydromorphic and subaqueous soils.	As above and in rivers and lakes.
Calcite and dolomite [$CaCO_3$]; [$CaMg(CO_3)_2$]	White	Calcareous soils.	Low rainfall regions.
Gypsum [$CaSO_4\ 2H_2O$]	Very pale brown	Saline soils and saline acid sulfate soils.	Low rainfall regions.
Quartz [SiO_2]	Light grey	Sandy soils.	All landscape positions.
Al hydroxide (gibbsite) $Al(OH)_3$	Transparent to white	Strongly hydromorphic and subaqueous soils.	Seeps and bottom lands.

†Occurring only in specific soil horizons or sedimentary units.

*Widespread occurrences in sandy and peaty sulfuric materials in South Australia (Fitzpatrick *et al.* 2000)

Sulfidic materials that form in acid sulfate soil landscapes (particularly as monosulfides in drains) can also act as a sink for metal contaminants, through trace element 'pyritization' (Burton *et al.* 2006b; Harbison 1986c; Huerta-Diez and Morse 1992; Morse and Luther 1999). The formation of sulfides and monosulfides can also improve water quality by consuming acidity (Burton *et al.* 2007).

Apart from micromorphological studies (Chapter 11) and cursory XRD investigations by Fitzpatrick and Self (1997), few detailed mineralogical studies involving XRD have been conducted in disturbed sulfuric and hypersulfidic materials from coastal Mediterranean type environments in Australia. Rapidly precipitating and dissolving minerals have also been identified in a wide range of disturbed inland acid sulfate soil environments from: **(i)** naturally and anthropogenically caused eroding stream-lines and drains in the Mount Lofty Ranges (Fitzpatrick *et al.* 1996b; Fitzpatrick *et al.* 2000; Fitzpatrick and Self 1997), and **(ii)** lowering of water levels in rivers, lakes and wetlands in the Murray-Darling Basin (MDB) caused by changing climatic environments (drought triggered and winter rainfall events; (Fitzpatrick *et al.* 2008b; Fitzpatrick *et al.* 2008c; Thomas *et al.* 2009)).

10.2. Materials and Methods

10.2.1. Background (experimental drains)

Numerous drains had previously been excavated at the Gillman study site, mainly to facilitate movement of storm water runoff from roads and buildings (Figure 10-2). Fortuitously, the vast majority of these drains transected only minor areas of sulfuric materials and hypersulfidic materials. This was due to the drains being aligned along (or utilised) former water courses in low lying areas that were dominated by calcareous and clay rich soils (classifying as hyposulfidic materials). The sandy soils that occur at higher relief areas (i.e. back barrier sand facies) and contain abundant sulfuric and hypersulfidic materials were therefore avoided. However, in 2005 land managers of the Gillman area proposed to re-align a major storm water drain that links the Range Wetlands (near Focus area A) with a large stormwater ponding basin in the northeast corner of the Gillman area, at Gillman Focus area C (Figure 6-11, Figure 7-2), and potentially to the Barker Inlet. The proposed re-alignment of the drain was to facilitate

development of the Gillman area for industrial purposes (Ruan Consulting 2006), and would require a new drain (about 1.3 km long and 2 to 3 m deep) to be cut through the most elevated parts of the Gillman site, which contained sulfuric and hypersulfidic materials (i.e. through the middle of the Overshoot Area; containing soil map units 5 and 6) (Figure 7-2). It was considered (by the author) that acid sulfate soils would pose significant acidity and metal mobilisation hazards to drain water quality, down gradient environments and (drain) infrastructure.

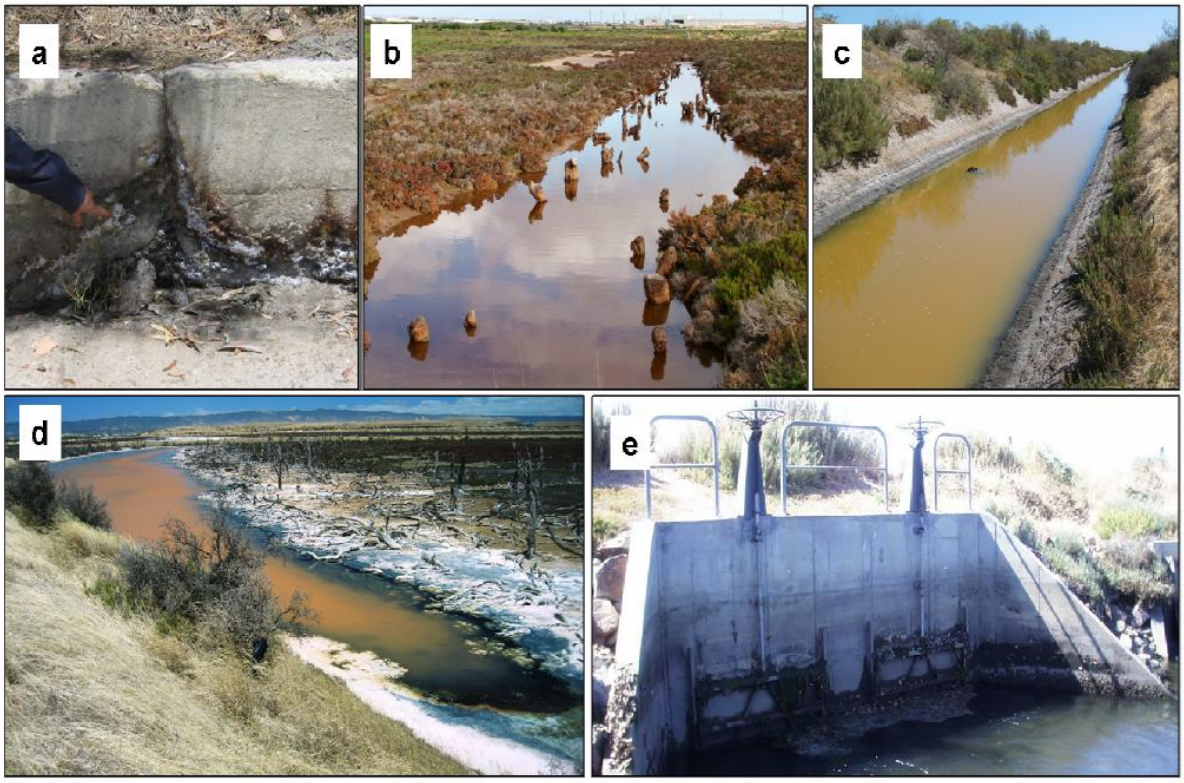

Figure 10-2 drain infrastructure at Gillman showing: (a) concrete corrosion in a lined drain (b, c) iron flock in a number of extensive, un-lined, open drains (d) iron flock in a large water filled stranded tidal creek (stormwater ponding basin) at Gillman and (e) tidal floodgates linking a bunded section of the Gilman area to North Arm Creek and the Barker Inlet.

To assess the impact that constructing a new drain would likely have on drain water quality, a relatively short (100 m long) experimental drain was excavated (up to 1.8 m deep) at Gillman Focus area A. The experimental drain was excavated during August 2002, and traversed soils containing sulfuric and hypersulfidic materials (Figure 10-3), similar to soils located along the route of the proposed drain. The experimental drain traversed from upland areas (map units 5 and 6) to low lying areas (map units 3 and 1). Soil profile BG 15 was located on the side wall of the experimental drain (Figure 10-3).

The Gillman study area (Figure 6-1) offered several unique advantages for investigating seasonal variation in field precipitation and dissolution of minerals in experimental, open drains. First, reactive soil solutions could be observed and sampled directly as a function of time during dissolution/precipitation processes. Second, the whole of the drain bottom is flat and exposed to the reactive drain water, making it a reasonable assumption that the entire drain floor surface is available for mineral growth or dissolution. Third, the range of precipitating minerals could be sampled to identify their composition. Fourth, the total volume of water present in the drain and infiltrated into the drain could be estimated, making it possible to determine the chemical flux and amounts gained or lost to mineral precipitation/dissolution.

In this chapter the experimental drain was used to investigate changes in geochemical and mineralogical processes and evaluate seasonal impacts on drain water quality (Figure 10-2). Conceptual soil-regolith models were constructed to better describe the results and implications of constructing drains through sulfuric and hypersulfidic materials for the land managers of the Gillman area.

Figure 10-3 (a) and (b) excavation of experimental drain (16th August 2002) in acid sulfate soil with sulfuric material and hypersulfidic material to investigate changes in geochemical and mineralogical processes as part of a series of management trials in the Gillman Focus area A. Image (a) shows a drain excavated in sandy soils typical of map unit 5 (e.g. soil profile BG 15) and 6 (e.g. soil profile BG 11). Image (b) shows Prof. Delvin Fanning holding a sample of sulfuric material exhumed from a drain in salt scalded mud flats, typical of map unit 3. The drain wall depicted in image (b) was described as soil profile BG 17.

10.2.2. Sampling

Surface water was sampled form the experimental drain on three occasions for bulk chemistry and minor elements: **(i)** the week following excavation of the drain (22nd August 2002), **(ii)** during summer (18th February 2003), while salt efflorescences on drain walls were abundant, and **(iii)** during winter (8th July 2003) following wet periods when salt efflorescences on drain walls were minor. Detailed water sampling and analytical methodologies used were described in the previous chapter (Chapter 9). Salt efflorescences were sampled from along the drain wall during summer 2003. Salt samples were taken from different levels at and above the drain water level, adjacent to soil profile BG 15 (Figure 9-13).

10.2.3. X-ray diffraction

Selected soil and salt efflorescence samples were analysed for mineralogy using X-ray diffraction (XRD) and scanning electron microscopy (SEM). Soil and salt samples were collected from soil profiles along the experimental drain during August 2002 when it was excavated and during the following summer (February 2003) when water levels were at their lowest (e.g. soil profiles BG 11, BG 15 and BG 17).

Soil or salt efflorescence samples were ground in an agate mortar and pestle and either back-pressed into steel holders or deposited onto Si low background holders (depending on how much sample was available). XRD patterns were recorded with a PANalytical X'Pert Pro Multi-purpose Diffractometer using Co K-alpha radiation, variable divergence slit, post diffraction graphite monochromator and fast X'Cellerator Si strip detector. The diffraction patterns were recorded in steps of 0.05° 2 θ with total counting time of 30 minutes, and logged to data files for analysis using HighScore Plus.

10.2.4. Scanning electron microscopic (SEM) analysis

Specimens were selectively sub-sampled to show the appropriate phases, often fractured to expose fresh surfaces, and then oriented and mounted onto aluminium specimen mounts using "Araldite" 5-minute epoxy resin. The samples were subsequently dried in a vacuum desiccator overnight, had the surfaces blown clean using a nitrogen jet, and were then coated with a conductive layer. Where imaging of the composition was

required, specimens were evaporatively coated with 30 nm of carbon, using an EmScope SC500 coating unit to provide electrical conductivity, and to maximize back-scattered electron (BSE) phase contrast. Carbon coating also minimizes extraneous x-ray peaks from the characteristic x-ray spectrum. Specimens were placed in a “Phillips” XL30 FEG-SEM, with an attached “EDAX” DX4 energy dispersive x-ray system. Sample examination was done using a primary electron beam energy of 20 KeV. Imaging was performed using the secondary electron (SE) signal where information about surface topography was required. Primarily, the SE signal carries information about the local topography of the sample because the signal is dependent on the angle of incidence of the primary beam.

Imaging was also performed using the BSE signal in cases when information about composition and phase were required. The backscattered electron signal primarily carries information about the average atomic number and the density of the sample commonly called "atomic number contrast or Z contrast". The characteristic x-ray signals were also collected at selected positions for qualitative energy dispersive x-ray (EDX) analysis. EDX analysis is possible within the volume over which the electron beam interacts (approximately four cubic micrometers), for all elements of atomic number greater than 6 with detection limits in the order of 0.1 to 5 wt % depending on the energy of the characteristic x-ray line.

10.2.5. X-ray fluorescence (XRF)

Selected salt efflorescence samples were analysed for trace elements by XRF. Approximately 4g of oven dried (105°C) sample was ground using a mortar and pestle and then mixed with 1g of Licowax binder. The mixture was pressed to 10 tonnes with a boric acid backing and the resulting pellet analysed on a Spectro X-Lab 2000 energy dispersive XRF system using Pb X-ray tube and 5 secondary excitation targets.

10.3. Results and discussion

10.3.1. Drain (surface) water

Surface water was sampled on the 22nd August 2002, the week following excavation of the drain, to provide a baseline from which to relate the evapo-concentration of elements, and repeated the following summer (February 2003) and subsequent winter (July 2003) (Table 10-2).

Laboratory pH measurements of water collected from the drain in August 2002 measured 3.12. The pH of drain water dropped more than 1 pH unit by the end of summer 2003, when pH measured between 1.95 and 2.14. Drain water collected during winter 2003 had higher pH (ranging between 2.98 and 3.02). The EC of drain water initially measuring an EC of 91.7 dS/m and increased considerably during summer months (measuring up to 183.2 dS/m in February 2003) and then decreased to 96.5 dS/m during winter (by 7th of July 2003).

The maximum concentration of chloride, sulfate and acidity followed a similar trend to EC during the separate sampling events, along with other elements such as Fe and Al, B, Ca, K, Mg, Mn, Na and Si (Table 10-2). Trace elements Cd, Cr, Cu, P, Pb and Zn remained below detection limits for the separate sampling periods (Table 10-2).

These trends were greatly influenced by evaporation of drain waters during summer months, which were coincident with considerably lower (> 60 cm) water levels in the drain (Figure 10-4), as well as the staged precipitation of salt efflorescences (Figure 10-5).

Table 10-2 results of chemical analyses of drain water during three separate sampling periods. Summer 2003 sampling episode was performed using peeper (peeper no. P2) (refer to Figure 10-5).

PARAMETER (Surface water)	WINTER 2002	SUMMER 2003	WINTER 2003	D.L.
pH	3.12	1.95	2.98	<0.01
Conductivity (EC) (dS/m)	91.7	183.2	96.5	<0.1
Chloride (mg/L)	42,958	171,767	59,703	<1
Sulfate (mg/L SO_4^{2-})	11,800	34,000	13,200	<10
Bicarbonate (mg/L $CaCO_3$ equivalent)	0	0	0	<10
Acidity (mg/L $CaCO_3$ equiv)	3,000	12,500	3,200	<100
Al (mg/L)	330	1500	610	<2
B (mg/L)	18	64	20	<2
Ca (mg/L)	1100	260	750	<10
Fe (mg/L)	54	1370	565	<2
K (mg/L)	830	3100	890	<10
Mg (mg/L)	3600	14000	4340	<10
Mn (mg/L)	12.0	48.0	18.0	<0.2
Na (mg/L)	26000	110000	30380	<10
S (mg/L)	4300	13000	5490	<10
Si (mg/L)	28.0	57.0	36.0	<0.2
Cd (mg/L)	<0.2	<0.2	<0.2	<0.2
Cr (mg/L)	<0.2	<0.2	<0.2	<0.2
Cu (mg/L)	<0.2	<0.2	<0.2	<0.2
Ni (mg/L)	<0.4	<0.4	<0.4	<0.4
P (mg/L)	<2	<2	<2	<2
Pb (mg/L)	<0.2	<0.2	<0.2	<0.2
Zn (mg/L)	<0.2	<0.2	<0.2	<0.2

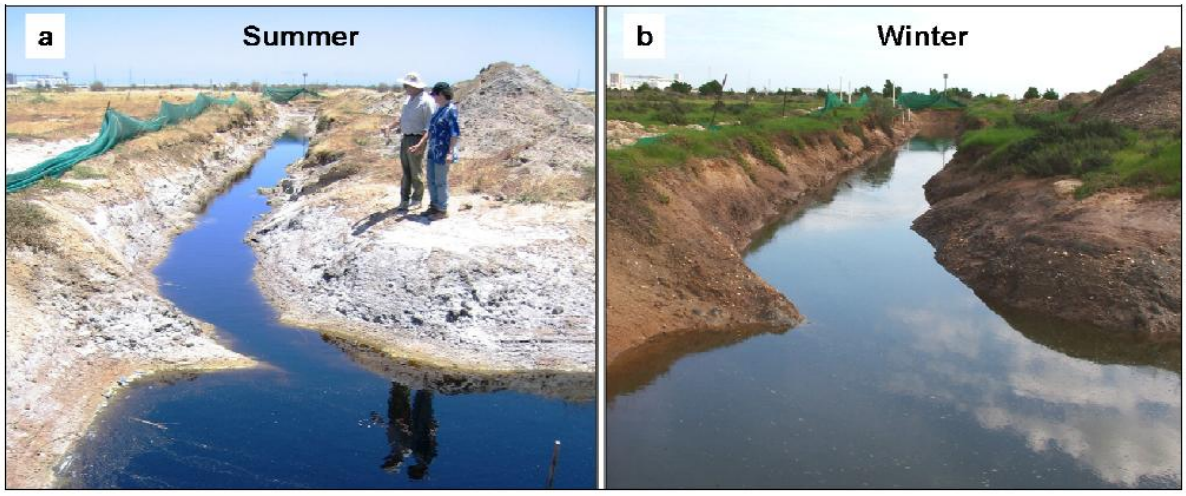

Figure 10-4 Photographs during: (a) summer (February 2003) with precipitation and accumulation of salt efflorescences on drain walls through element concentration at the surface by capillary action and evaporation and (b) winter (July 2003) with dissolution of most salt efflorescences and subsequent flow into the drain water. This site is seen subsequent to that initially (Figure 10-3(a) after excavation in August 2002).

Although the EC of surface water in the drain essentially doubled during summer, the concentration of most elements (Na, Cl, Al, Mg, Mn etc.) and acidity [H^+] increased by a factor of four. The Fe concentration of drain water increased by a factor of 24 (Table 10-2). The Cl^- to SO_4^{2-} mass-ratio changed from 0.27 in August 2002 to 0.20 in summer 2003, indicating enrichment in SO_4^{2-} between seasons and significant enrichment of SO_4^{2-} compared to the ionic mass-ratio in seawater (Cl^-:SO_4^{2-} = 7.2). The subsequent increase in the Cl^- to SO_4^{2-} mass-ratio from 0.20 in summer to 0.22 in following winter suggests that some sulfide formation occurs when water levels in the drain rise. The Ca concentration of drain water was lower during summer, due to the increased acidity.

10.3.2. Salt efflorescences

Salt efflorescence crusts and blooms formed along exposed walls of the drain during summer months (Figure 10-5). The location of salt efflorescences on the drain walls provided an indication to the conditions of formation, as drain water pH and EC changed proportionally to the height (volume) of the water in the drain. The chemical properties of soil layers hosting the salts at different levels on the drain walls changed with depth down the profile (e.g. BG 15) and would have influenced salt efflorescent mineralogy. Soil chemical data for profile BG 15 is provided in several previous chapters of this thesis. In the near surface layers (50 to 80 cm) on the drain walls (Area c1, Figure 10-5) clay and carbonate contents were relatively high and sulfate salts formed as a 1 mm thick white “fluffy” crust dominated by gypsum, halite, goethite and tamarugite (Figure 10-5 and Table 10-3). Lower layers on the pit face (Area c2; 80 to 100 cm), soil solutions were more acidic (pH < 2) allowing thicker (2-20 mm) accumulations of gold, cream, white and orange coloured salts that included mixtures of: sideronatrite, tamarugite, pentahydrite, starkeyite, hexahydrite and gypsum (Figure 10-5 and Figure 10-6). Significant quantities of acidic (pH < 1) sulfate-rich salts accumulated under sheltered overhangs at a number of deeper locations along the drain wall (e.g. Area c3; 100 to 120 cm) as white gels (10-30 mm thick) that were covered by a yellow crust (5 to 10 mm thick). This material consisted of pyrite that oxidised and release sulfate, Fe and acidity. The acid dissolved weatherable minerals to form a white gel containing tamarugite, gypsum, melanterite, metaalunogen and hexahydrite, and then formed a yellow surface crust containing tamarugite, gypsum and hexahydrite) (Figure 10-5 and Figure 10-6).

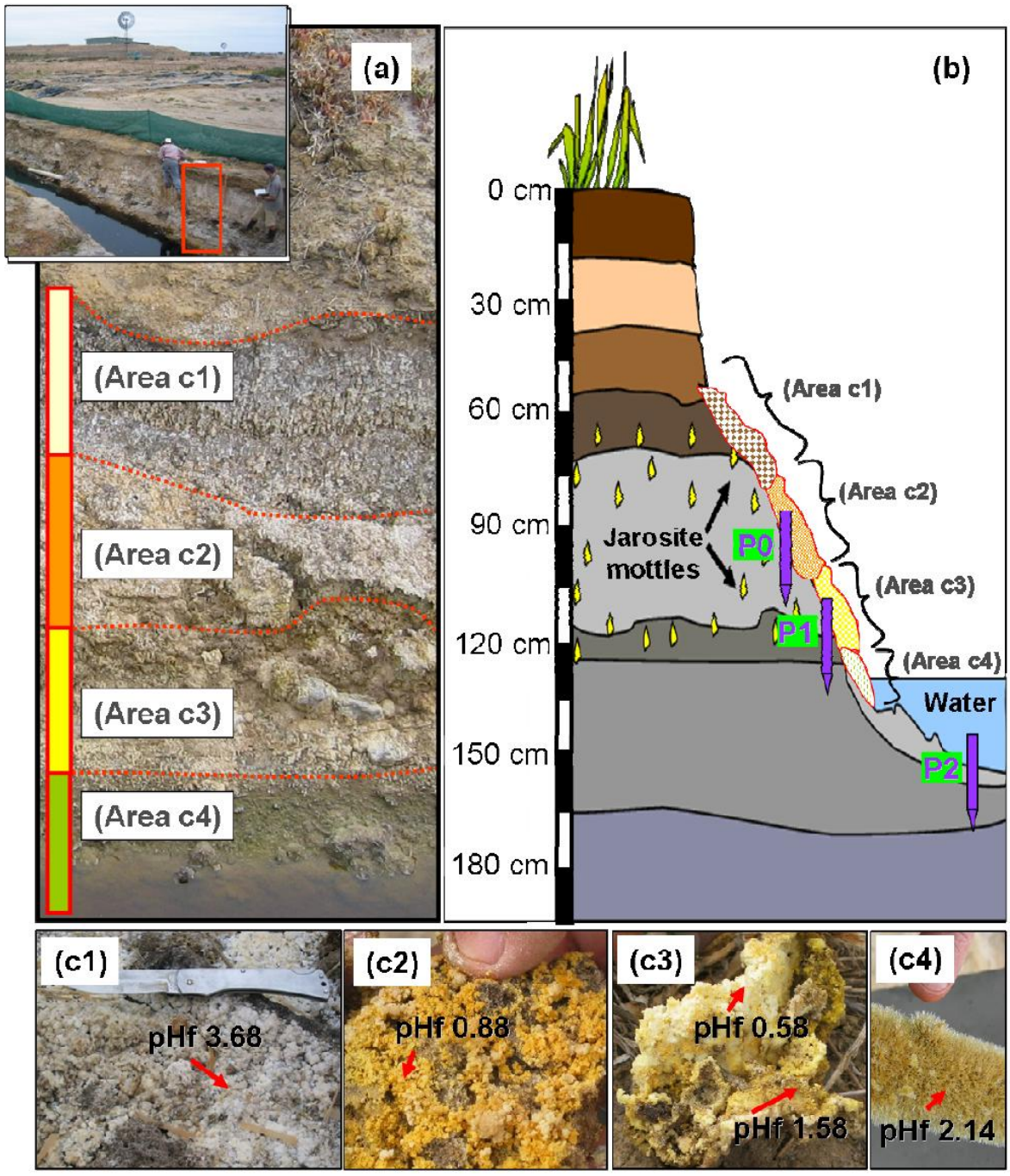

Figure 10-5 Schematic cross section through drain showing photographs of the acid sulfate soil profile and sulfate-rich salt efflorescences occurring on exposed drain wall at Gillman, focus area A. Where: (a) annotated photo of the drain wall (inset) and showing the areas (Area c1 to Area c4) where groups of salt efflorescences occurred. (b) schematic cross section of drain wall showing soil layers of profile BG 15, and where groups of coloured salt efflorescences precipitated. (c1-c4) photographs of salt efflorescence samples collected for XRD analysis. Refer to Table 10-3 for mineral occurrences. Peepers (P0-P1) collected pore waters from within salt blooms.

At and below the level of the acidic drain water (Area c4; 120 to 140 cm) euhedral gypsum crystal laths (2 mm long) had precipitated on the surfaces of soils. The gypsum samples also contained halite and hexahydrite (i.e. pyrite oxidised to form gypsum and hexahydrite in Area c4) (Figure 10-5 and Table 10-3). The green tinge of salts at Area

c4 may be due to algae and possibly minor occurrences of melanterite, which were not identified by XRD in this sample. Alpersite, which is defined as the Mg-dominant phase of the melanterite group (Peterson *et al.* 2006) may have also occurred within melanterite-bearing samples, given the high Mg concentration of drain and pore waters.

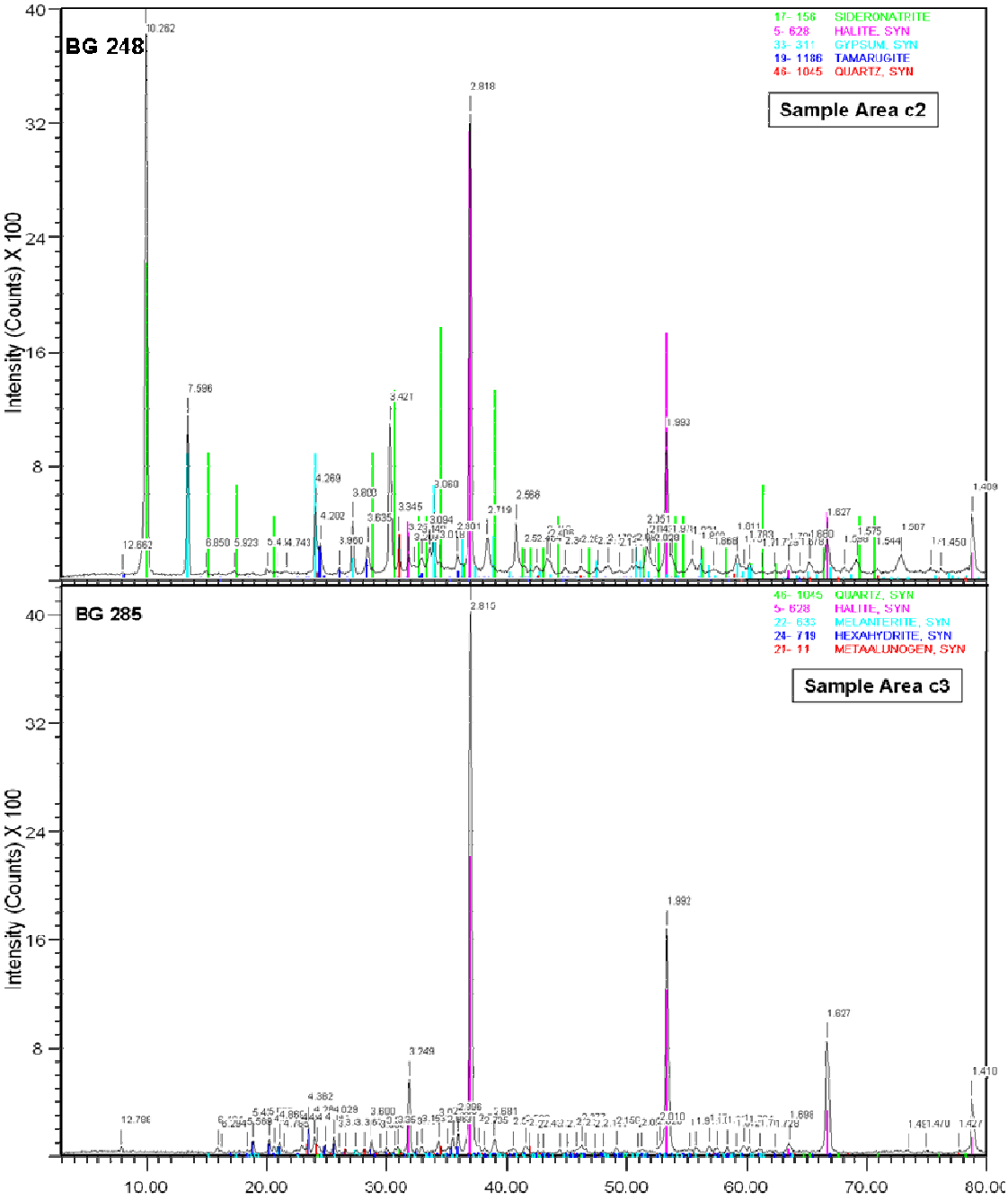

Figure 10-6 X-ray diffractograms for two salt efflorescence samples collected from the wall of the experimental drain, adjacent to soil profile BG 15. These XRD document the first occurrence of sideronatrite [$Na_2Fe(SO_4)_2(OH).3H_2O$], tamarugite [$NaAl(SO_4)_2.6H_2O$] and (meta)alunogen in coastal acid sulfate soils in Australia.

Blödite was identified by XRD (Table 10-3) in a salt crust sample collected from the surface of a salt scalded area adjacent to the drain shown in image (b) of Figure 10-3, at soil profile BG 17. Selected X-ray diffractograms and semi-quantitative EDX graphs and SEM photomicrographs of salt efflorescence samples are displayed in Appendix G.

Table 10-3 Minerals identified by XRD in salt efflorescences (X-ray diffractograms for 2 samples are displayed in Figure 10-6 and others in Appendix G). Refer to Figure 10-5 for images of the salt samples that occupied the various areas on the drain wall.

Mineral	Formula	Colour	Area on drain wall
blödite	$Na_2Mg(SO_4)_2.4H_2O$	yellow	Surface of salt scalded area
goethite	FeOOH	strong brown	c1, c2
halite	NaCl	white	c1, c2, c3, c4
gypsum	$CaSO_4.2H2O$	white to pale brown	c1, c2, c3, c4
tamarugite	$NaAl(SO_4)_2.6H_2O$	yellow	c1, c2, c3
pentahydrite	$MgSO_4.5H_2O$	green	c2, c3
jarosite	$KFe_3(SO_4)_2(OH)_6$	yellow	c2, c3
sideronatrite	$Na_2Fe(SO_4)_2(OH).3H_2O$	reddish yellow	c2, c3
starkeyite	$MgSO_4.4H_2O$	cream	c2, c3
hexahydrite	$MgSO_4.6H_2O$	white	c2, c3, c4
metaalunogen	$Al_4(SO_4)_6.27H_2O$	white	c3
melanterite (alpersite)	$2Fe^{2+}(SO_4)_2.7H2O$	green	c3

10.3.3. Formation of salt efflorescences

Salt efflorescences are formed by oxidation of iron sulfides and weathering of minerals in the exposed soil profile, followed by wicking and evaporation of acidic soil solutions (pH < 4) containing Na, Cl, Fe, S and other elements to the soil surface. Some of the sulfuric acid produced during pyrite oxidation reacted with the surrounding silicate and alumino-silicate soil minerals to release cations (e.g. Ca, Al, Zn, K, Mg, Mn and Ni) into solution. These cations were elevated in soil solutions collected by peepers positioned within the salt efflorescent blooms at in the drain wall (Table 10-4). Other minor elements identified in pore water solution included Cr (11-27 mg/kg), Ni (15-20 mg/kg), Sr (15-23 mg/kg) and Zn (4-11 mg/kg). Trace elements Cd, Cr, Ni and Zn were below detection limits for drain waters (Table 10-2).

The formation of goethite in the upper portion of the drain wall profile (Area c1 and above) is likely due to the higher pH of soil solutions, being controlled by higher carbonate and clay contents. During winter, drain water was in contact with Area c1, but the pH of the water was usually above 3 at that time. The precipitation of goethite leads to the removal of Fe from soil solution and allows Mg salts (e.g. starkeyite, pentahydrite and hexahydrite) to dominate at lower positions on the drain wall. Iron oxides (e.g. schwertmannite) did not precipitate below Area c1 because soil and water pH was less than 2.5. The down-profile movement of Fe and other elements in soil solution is evident when comparing the peeper samples from Area c2 and Area c3 (Table 10-4). Iron content of drain water (probably Fe^{3+} considering redox conditions were oxidising) was considerably higher during summer (1370 mg/L) than in winter (565 mg/L), which may explain the occurrence of melanterite at a low position on the drain wall, Area c3. The high Fe content of drain water during summer may be influenced by the oxidation of sulfides when summer water levels dropped below Area c3, exposing soil layer 5Bigj in profile BG 15, which had a S_{CR} content of 6.88% (Figure 10-7). The dissolution of iron sulfate minerals can also promote pyrite oxidation, as ferric iron oxidises pyrite faster than dissolved oxygen in aqueous systems (McKibben and Barnes 1986; Williamson and Rimstidt 1994).

In Area c3, a white Al gel (containing metaalunogen) occurred below a yellow iron sulfate crust (containing jarosite and sideronatrite) (Figure 10-5 and Table 10-3). This indicates that the activity of Al became higher relative to iron as iron was removed from solution while jarosite and sideronatrite precipitated. The Al content of drain water was similarly concentrated (1500 mg/L) during summer months, explaining the formation of metaalunogen at Area c3 (Table 10-3). The occurrence of tamarugite and metaalunogen at the most acidic sites in the drain wall (Area c2 and Area c3) was expected as these salt efflorescences contain additional (retained) acidity (refer to Figure 9-14) in the form of Al^{3+}, which is not detected by a pH meter. The impact on water quality from each mineral phase is therefore different. Minerals bearing trivalent cations (e.g. jarosite, metaalunogen and tamarugite) release the most acid due to hydrolysis of ferric iron and aluminium, however jarosite is relatively insoluble, particularly within this low pH environment. Ferrous iron also undergoes hydrolysis, to a lesser extent, so that sideronatrite and melanterite are less acidic, but further hydrolysis will occur in aqueous environments, causing a latent release of acidity (Jambor *et al.* 2000).

Gypsum and halite occur at all positions on the drain wall profile, but do not present an acidity hazard to drain waters. The occurrence of gypsum indicates that carbonates are being dissolved in this acidic environment. Halite is a product of evaporating brines of marine origin. Gypsum and halite are the last salts to precipitate, with halite being the most soluble salt.

At this site, salt efflorescence mineralogy involved oxidation reactions, hydration and dehydration reactions and hydrolysis, acidification and neutralisation reactions. The composition of drain water and pore water was a major factor controlling the mineralogy of salt efflorescences, with some influence by the parent mineralogy of the soil profile. The relative position (elevation) that salts occur on the drain walls is related to solution chemistry of the adjacent soil and seasonal changes in drain water EC and pH. Sulfuric acid concentrations increased as ferric sulfate rich solutions evaporated.

The salt efflorescences sampled have potential to impact the quality of receiving waters at this site. The Fe^{3+} and Al^{3+} rich salts, common in Area c2, would produce the most amount of acidity upon dissolution. This is also evidenced by retained acidity measured in soil samples from profile BG 15, relative to this position in the drain (Figure 10-7). The load of trace elements in drain waters would likely be minimal, in this case, due to large a dilution factors.

Table 10-4 Chemistry of pore water samples collected using peepers from within salt blooms from Area c2 (peeper P0) and Area c3 (Peeper P1) (refer to Figure 10-5). The samples were collected using peepers (refer to Chapter 9 for sampling methodology). Pore waters sampled from within and immediately below salt crusts at Area c2 and Area c3 were elevated in (B, Cr, Mn, Ni, Si, Sr and Zn) when compared to pore water sampled from deeper below the salt efflorescences (Figure 9-13) or compared to the drain water (Table 10-2 and Figure 9-16). The concentration of trace elements from within the salt crusts themselves (Table 10-5) was similar to that of the contacting pore water samples listed here, with a few exceptions: (i) Mn, Sr, Cu and Zn were slightly more concentrated in the salts, and (ii) Ni was lower in the salts than in the pore waters.

Sampling area	**Area c2 (Peeper P0)**		**Area c3 (Peeper P1)**		
	Pore water sampling increment (distance from salt surface)				
Parameter	**0-1 cm**	**2-3 cm**	**0-1 cm**	**2-3 cm**	D.L.
pH	1.84	1.62	2.31	1.94	0.01
EC dS/m	77	53	102	102	1
Cl mg/L	78000	50100	123000	131000	10
Al mg/L	4200	2000	2300	3100	10
B mg/L	62	29	95	130	1
Ca mg/L	370	580	170	150	10
Cd mg/L	<0.5	<0.5	<0.5	<0.5	0.5
Cr mg/L	16	27	11	11	1
Cu mg/L	<0.5	1.7	2.0	2.0	0.5
Fe mg/L	830	760	1600	2200	10
K mg/L	150	60	2700	3600	10
Mg mg/L	12000	4000	20000	25000	10
Mn mg/L	137	38	83	97	1
Na mg/L	56000	27000	62000	63000	10
Ni mg/L	20	15	15	15	5
P mg/L	<5	<5	<5	<5	5
Pb mg/L	<0.4	<0.4	<0.4	<0.4	0.4
S mg/L	20700	7450	20800	25800	10
Si mg/L	44	56	44	57	1
Sr mg/L	18	15	23	19	1
Zn mg/L	11	4	9	10	1

10.3.4. Storage of trace elements

The paragenesis of sulfate salt efflorescences can assist understanding of their environmental impact because evolving sulfate mineralogy affects the acidity and trace metal load of runoff solutions. The precipitation of hydroxysulfates and oxyhydroxides of Fe and Al, to some extent, may attenuate drainage waters by scavenging associated trace elements through processes of adsorption and /or co precipitation (Bigham and Nordstrom 2000). Therefore salt efflorescences also have the potential to pollute upon dissolution (Jerz and Rimstidt 2003).

Salt efflorescence samples were selected from 5 different positions on the walls of drains and analysed for trace elements by XRF. The results indicated that concentrations were above 100 mg/kg for As, Ba, Br, Ce, La, Mn, Mo, Sr and V in one or more of the samples (Table 10-5). Contaminated soils were common in the Gillman area (refer to Chapter 9) and were a likely source for some of the trace elements in the salt samples. Trace elements that were elevated in the soils (e.g. profile BG 15) represented a similar suite of trace elements to those elevated in the salt efflorescence samples (Table 10-5). Relative to deeper soils in profile BG 15, near surface soil samples had elevated levels of As, Ba, Cr, Cu, Mn, Ni, Pb, Sr, V and Zn, while concentrations of Br and Mo increased with depth (Figure 9-13). Compared to the contacting surface soil layers in the drain wall, salt efflorescent samples generally contained higher concentrations of trace elements (Figure 10-7 and Table 10-5).

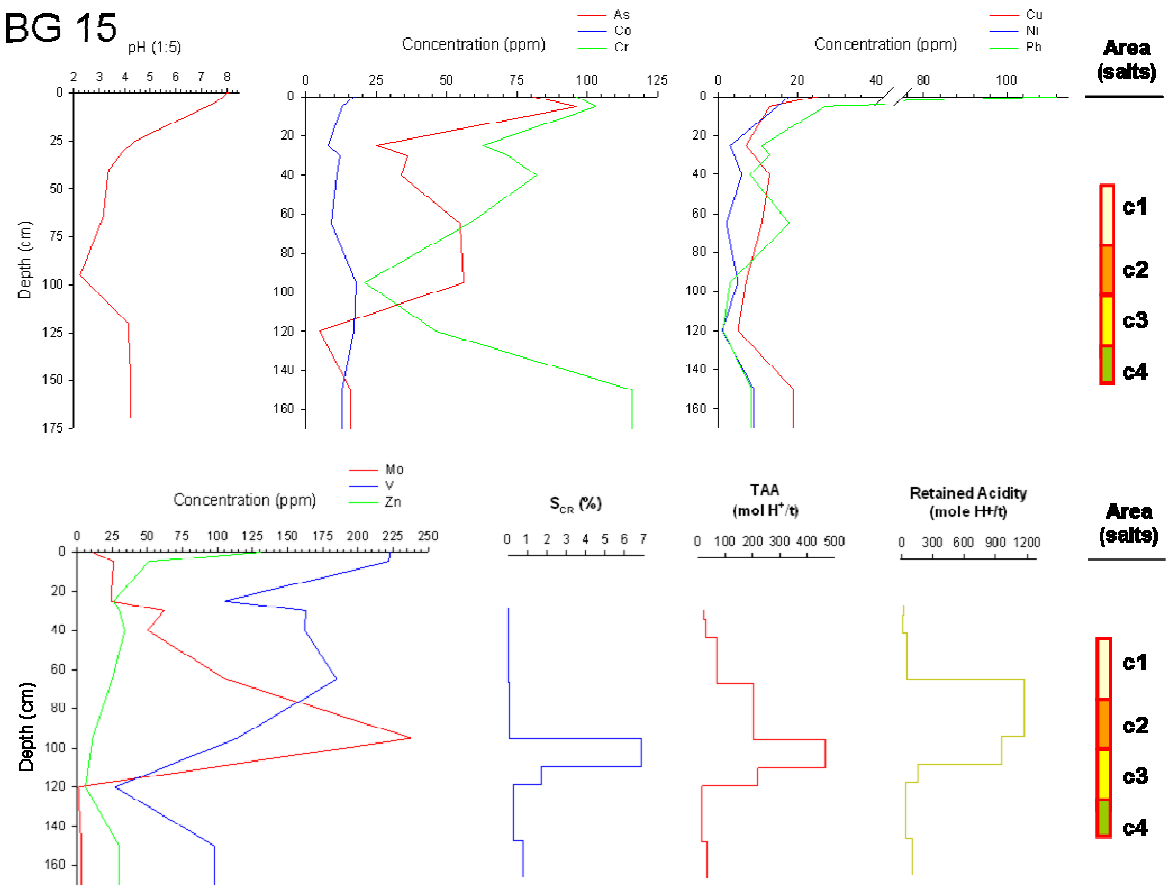

Figure 10-7 Down profile soil pH, trace element and acid sulfate soil characteristics of profile BG 15.

Table 10-5 Trace elements determined by XRF for selected salt efflorescent samples. Green highlighted cells indicate where the trace element concentration is higher in the salt sample than within any of the soil samples from either profile BG 15 or BG 17.

	Sample ID					DL
	Salt crust	**Area c1**	**Area c2**	**Area c3**	**Area c4**	
Element	BG17-235	BG15-226	BG15-247	BG15-286	BG15-221	(mg/kg)
As	14	153	5	7	7	2
Ba	104	78	<12	<12	<12	12
Br	196	125	615	592	474	1
Cd	<4	<4	<4	<4	<4	4
Ce	22	69	<18	<18	395	18
Co	<5	6	5	6	<5	5
Cr	26	32	8	17	6	3
Cu	8	9	5	4	5	1
La	22	<16	<16	<16	131	16
Mn	231	26	338	282	60	8
Mo	9	980	<1	<1	2	1
Ni	4	<2	<2	7	<2	2
Pb	31	16	<3	<3	<3	3
Sr	71	20	73	112	1591	1
U	9	67	<2	<2	13	2
V	36	173	16	19	40	6
Zn	36	14	5	15	17	2
Zr	96	48	5	4	<1	1
Major salt minerals	halite, blodite	goethite	halite, tamarugite	halite, gypsum, tamarugite, hexahydrite	halite, gypsum, hexahydrite	

The salt sample from the surface crust of profile BG 17 was dominated by halite and blödite, and had elevated Ba, Mn, Pb and Zn with respect to the other salt samples. The Pb and Zn content of the salt sample were slightly higher than in the underlying soil samples from profile BG 17, but were still considerably lower than in the surface soil samples from profile BG 15. It is widely known that many of trace elements (e.g. Pb, Cd, Zn, and to a lesser extent Cu) may co-precipitate with halite (Stiller and Sigg 1990). In this case, it is likely that Pb and Zn was transported to the surface salt crust as wind blown dust from nearby industrial soils that were contaminated by these elements (e.g. topsoil of profile BG 15).

Goethite mottles that were hand picked from Area c1 along the open drain were particularly elevated in As, Cr, Cu, Mo and V, with respect to the other salt samples. These elements are likely to be anions in these layers. The As and Mo content of the goethite rich sample was higher than in any of the soil samples collected from the Gillman study site, the highest of which were from profile BG 5 (As of 140 mg/kg) and profile BG 15 (Mo 238 mg/kg) (Appendix E). Arsenic is also associated with P in soils.

The elevated Mo (238 mg/kg) found in bulk soil sampled from profile BG 15 was associated with a soil layer containing extremely high sulfide contents (S_{CR} of 6.88%). Molybdenum may enter solution as the oxyanion molybdate (MoO_4^{2-}), and exhibits similar behaviour to arsenate, being scavenged by Fe (Roy *et al.* 1986). Arsenic was also elevated in near surface soil samples from profile BG 15 (96 mg/kg) and showed a linear relationship with Cr (likely occurring as chromate) and V (likely occurring as vanadate) in topsoils from upland profiles at Gillman (refer to Chapter 9).

Metals may occur naturally within sulfides, however in this case it is more likely that the suite of trace elements (As, Cu, Pb, and Zn) within topsoils at Gillman was likely influenced by windblown, anthropogenic sources (e.g. in dust, fumes and ammunition shells), since they essentially blanket both tidal and reclaimed areas of the Gillman site (refer to Chapter 9). Arsenic and other trace elements occurring in near-surface soils of profile BG 15 may be relatively immobile due their incorporation in Fe oxides in a high pH environment (soil pH ranging from 7-8). Large seasonal fluctuations in redox conditions may provide a mechanism for trace elements to move down through the soil profile, and may also have implications to the toxicity of As (and Cr) in this environment. The reduced forms of As (As^{3+}) and Cr (Cr^{6+}) are more toxic than their oxidised forms (As^{5+} and Cr^{3+}) (Balasoiu *et al.* 2001).

A similar distribution of trace elements was observed in profile BG 11 where trace elements As, Mo, Ba, Br, Cr, Cu, V and rare earth elements (REE) (Figure 9-15) were elevated at the surface and in subsurface sulfuric materials that experienced reducing conditions seasonally (refer to Chapter 8). The Zn content of goethite sampled from Area c1 was similar to that of the contacting soil layers in profile BG 15 (26-30 mg/kg), but was considerably lower than the Zn content of the surface soil sampled from profile BG 15 (131 mg/kg). EDX analysis of a goethite mottle sampled from relic hyposulfidic material in profile BG 11 (at 45 cm depth) contained elevated Zn (6.4 wt.%) (Appendix G).

Salt samples from Area c2 (containing halite and tamarugite) and Area c3 (containing halite, tamarugite, hexahydrite and gypsum) had similar concentrations of Br and Mn, which were elevated with respect to the salt sampled from the other areas (Table 10-5). Mn oxides accumulate just above historic reduced layers. Mg-rich salts, such as

pentahydrite and starkeyite, which also occurred at these positions, can contain elevated Co and Zn (Romero *et al.* 2006).

Halite, gypsum and hexahydrite was identified in the salt efflorescence sampled from Area c4 (Table 10-5). This sample had precipitated directly from the drain water onto a plastic pipe used to house redox electrodes (Figure 10-5). This salt sample contained high concentrations of Br and extremely high concentrations of Sr and REE (Ce and La), relative to the other salts sampled from the drain (Table 10-5). Sr often precipitates as $SrSO_4$ with $CaSO_4$ or $MgSO_4$. REE were also identified by SEM-EDX using back-scattered-electron mode, in a salt crust containing blödite (La) and in a P-rich salt from soil profile BG 11 (Ce) (Figure 10-8). The distribution of Br in these salt samples (and in soil profile BG 15) is likely related to salinity, as Br often substitutes for Cl in halite (NaCl) and is concentrated in brines derived from sea water.

The negligible trace element concentrations determined in pore waters sampled from > 10 cm below the salt efflorescent blooms (e.g. sampled by peepers P0 and P1) suggest that the trace elements sequestered by the salts may have been from an alternate source, such as via down-profile migration with infiltrating waters and / or by windblown dust, depositing directly onto the salts in the open drain. Either way, salt efflorescences provide a pathway for trace elements to contaminate drain waters because they are able to both store metals and then dissolve in the hyper-acidic pore waters within a thin a 15 cm layer below where the salts had precipitated (Table 10-5 and Figure 9-15). However, Mo and V were likely sourced from the adjacent (contacting) soil layers.

Trace elements were not detectable in surface waters within the drain during summer or winter sampling periods (Table 10-2). This suggests that trace elements may be either: **(i)** entering the drain waters on dissolution but at concentrations too low to detect, or **(ii)** removed from drain waters by adsorption on poorly crystalline and amorphous layer silicate minerals forming in the water column and then deposited on the drain bottom. The adsorption mechanism seems unlikely as pore water samples from the drain bottom (e.g. in samples from peeper P2 (Figure 10-5) during summer contained no detectable trace elements (refer to Chapter 9). This could be further tested by analysing samples of bottom sediments from the drain by XRF and XRD analyses. Reduced redoximorphic features were not observed in the bottom sediments of the drain water during the course

of this study. However, it is possible that trace elements are being scavenged by sulfide minerals forming in soil layers in the drain walls. Another possible reason for the low concentration of trace elements in the drain waters may be due to scavenging (locking-up) by Fe and Mn oxides that occur in the top 70 cm of the drain profile (and includes area c1). The elevated concentrations of trace elements in salt efflorescences in Areas c2 and c3 may also be due to the downward movement of particulate matter from surface soil layers (e.g. as wind blown dust), being deposited on the surface of salt crusts. The amount of contaminated dust entering the drain water directly is evidently insufficient to elevate trace elements to detectable limits (due to dilution). If the trace elements in the dust are sorbed on crystalline Fe and Mn oxides, they may not dissolve in the acidic-oxidising conditions of the drain waters, but do in the hyper-acidic oxidising conditions of the salt efflorescences in Areas c2 and c3, where pH < 1 occurred (Figure 10-5).

Although trace element concentrations within the salts along the drain may have been influenced by wind-blown sources (e.g. from contaminated topsoils), some contaminants (e.g. Ba, Co, Cu, La) were observed *in-situ* in soil samples that were carefully excavated from soil profile BG 11 (Figure 10-8). Dissolution of trace elements in these environments would likely vary diurnally, in response to large diurnal fluctuations in Eh of up to 100 mV (refer to Chapter 8). Diurnal variations in stream water trace element concentrations have been coupled to diurnal fluctuations in pH (of up to 1 pH unit) arising from changes in photosynthetic and biological activity, and light intensity (e.g. Bourg and Bertin 1994; Fuller and Davis 1989). Blödite was identified by XRD in salt sampled from the surface of a salt scalded area adjacent to the drain, at soil profile BG 17 (Table 10-3). The salt sample containing blödite contained elevated La (9.36 wt.%), identified by EDX analysis (Appendix G). SEM images and EDX data of soil (sulfuric material) sampled from deeper in profile BG 11 (150 cm depth) identified elevated trace elements (Ba, Ce, Co and Cu, Figure 10-8), that occurred with salts: (a) barite ($BaSO_4$) grain, (c) cerium bearing phosphate ($CePO_4$) grain, and (e) a Cu and Co bearing sodium chloride (Cu,Co,NaCl) grain.

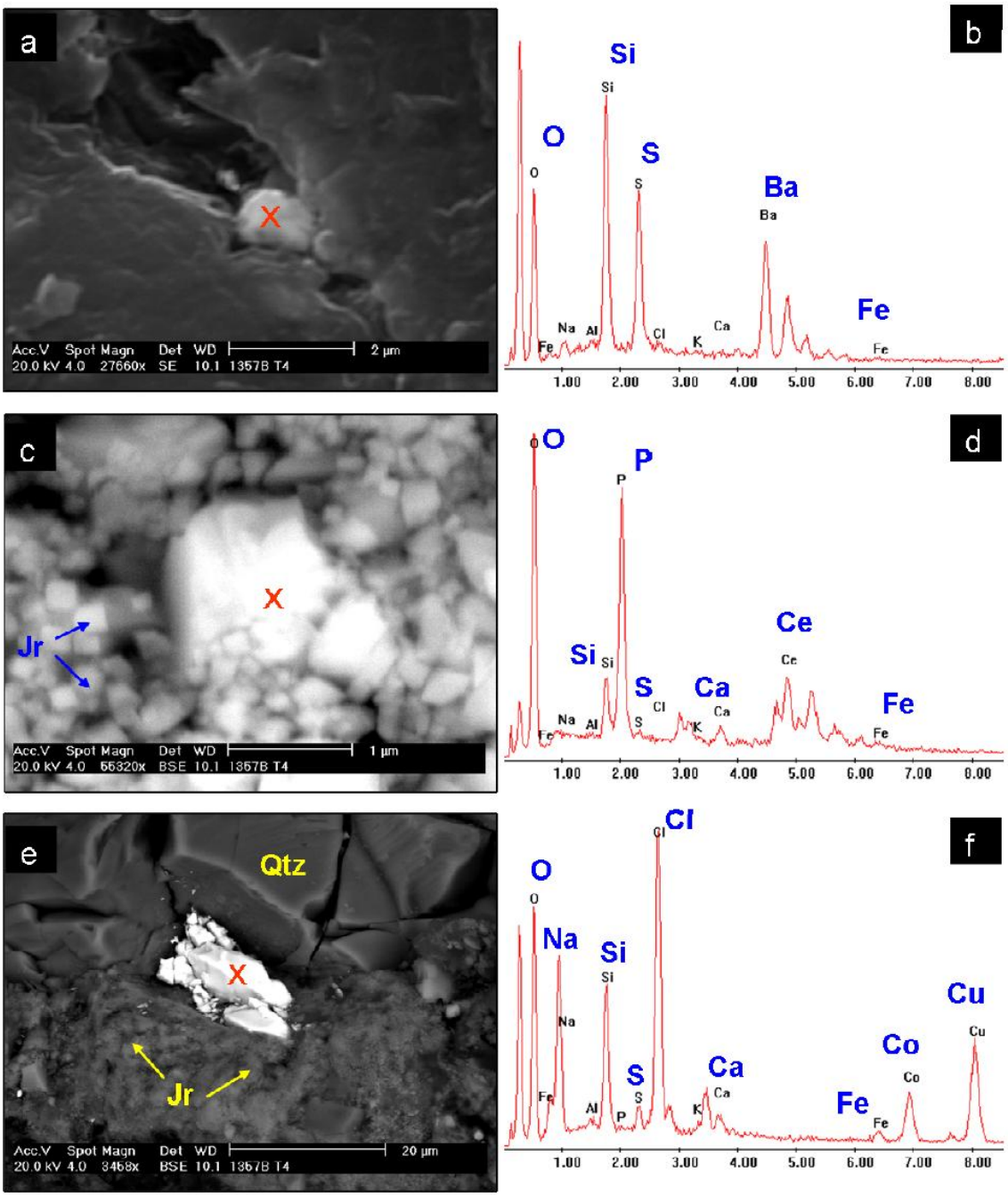

Figure 10-8 SEM images ((a) SE, (c) and (e) BSE) and EDX data for sulfate salts containing trace elements identified within soil samples (sulfuric materials) from soil profile BG 11, at 150 cm depth. Figure (a-b) shows a grain of barite. Figure (c-d) shows a phosphate mineral grain containing REE (Ce). Figure (e-f) shows a sodium chloride grain containing Cu and Co.

10.3.5. Trace elements associated with sulfide minerals

Acid sulfate soils with hypersulfidic materials, such as in intertidal mangrove environments, are a good conserver of trace metal contamination or mineralisation. Sulfidic material, and salt efflorescent samples may be a preferential sampling medium for mineral exploration as well as for identifying pollutant sources during forensic soil investigations (Skwarnecki *et al.* 2002). Contaminants were identified in sulfidic soil materials by SEM from two sites with similar characteristics to the Gillman and St Kilda study sites: **(i)** Garden Island (Fitzpatrick 1996), and **(ii)** Solomontown Island (Thomas and Fitzpatrick 2006b). The St Kilda Formation was the sampling medium at both sites.

At Garden Island, located in Barker Inlet and less than 1 km north of the Gillman study site, secondary sulfide minerals were associated with organic matter and were likely bio-mineralised with Pb and V (Figure 10-10). These elements were elevated in near-surface soil across the Gillman study site, including within intertidal areas (soil profiles BG 20 and BG 21, refer to Chapter 9). A copper sulfide (possibly chalcopyrite) grain was also identified in mangrove soils at the St Kilda study site and interpreted to be a preserved, primary chalcopyrite grain that likely originated from rock batters lining the near by St Kilda marina.

Figure 10-9 SEM (a) (SE) and (b) BSE showing lead bearing secondary sulfide minerals (PbS) formed on organic matter (OM) in an intertidal mangrove sediment from Garden Island, Barker Inlet (Fitzpatrick 1996). (c) EDX of the light grey coloured mineral occurring in (b) indicated with the red cross.

At Solomontown Island, located about 210 km north of Adelaide, primary minerals were likely airborne dust particles from the adjacent Port Pirie lead smelter and included euhedral galena and pyrite mineral grains and possibly sphalerite, arsenopyrite and

chalcopyrite (Figure 10-10). Secondary sulfide minerals were associated with organic matter and were bio-mineralised with Pb, Zn, As and Cu (Figure 10-10). Galena and sphalerite were also identified by XRD analysis of the sample (Thomas and Fitzpatrick 2006b).

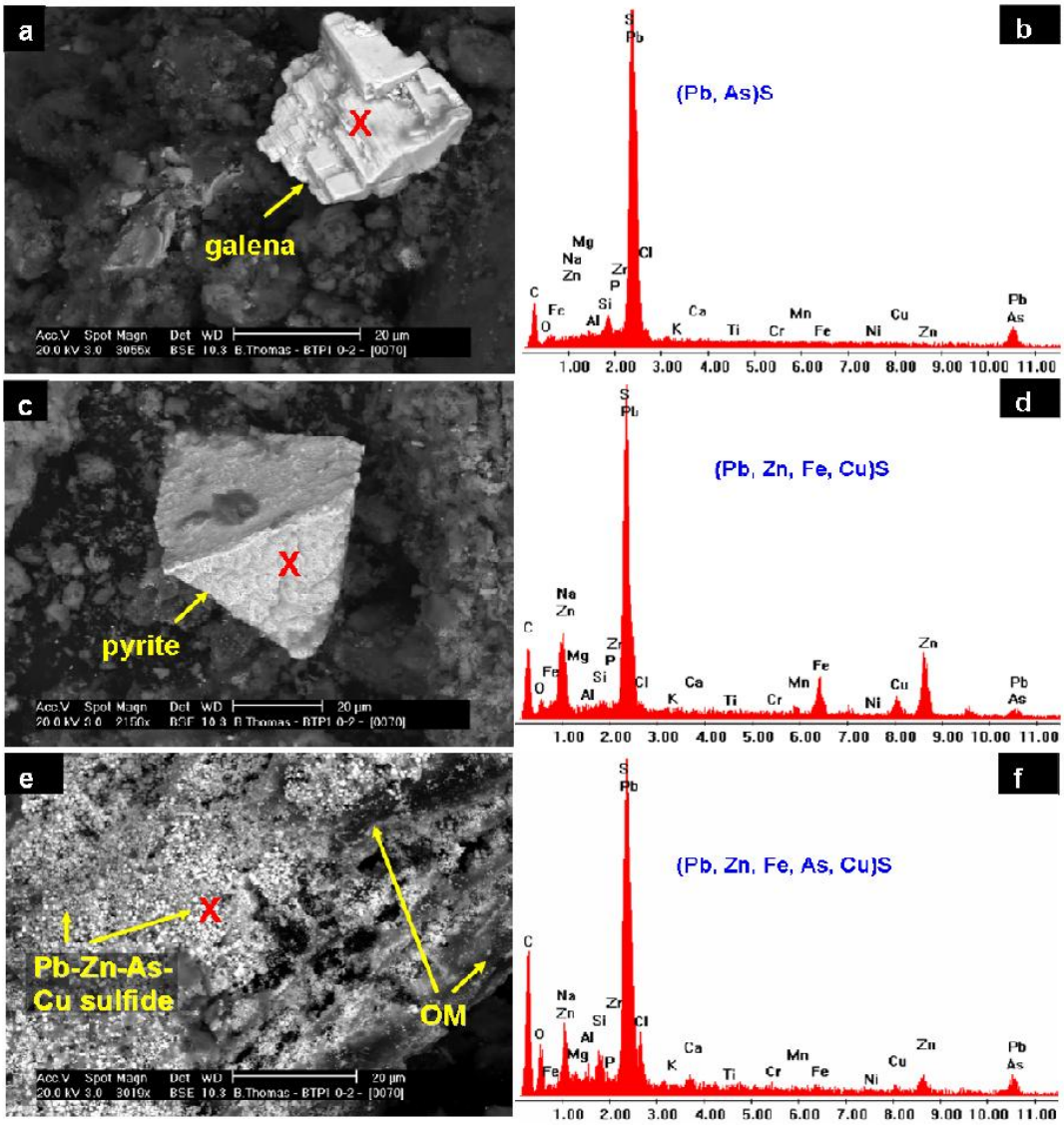

Figure 10-10 SEM (BSE) photomicrographs from near surface samples of an intertidal mangrove sediment at Solomontown Island showing (a) scanning electron micrograph showing bright euhedral crystal of lead-sulfide (galena). (b) EDX spectrum of euhedral galena crystal; containing Pb, S. (c) scanning electron micrograph showing light grey, euhedral crystal of altered Fe sulfide (pyrite). (d) EDX spectrum of euhedral sulfide crystal containing Pb, Zn, Cu and As; and possibly with associated secondary minerals of sphalerite, chalcopyrite and arsenopyrite. (e) scanning electron micrograph showing a mass of fine, bright crystals of lead sulfide (possibly pseudomorphs after framboidal pyrite) and are likely to be bio-mineralised sulfide minerals as they are closely associated with organic matter (remnant plant material showing cellular structure). (f) EDX spectrum of bio-mineralised sulfide mineral grains containing Pb, Zn and As bearing sulfides; probably galena, sphalerite and arsenopyrite.

10.4. Summary

Soil-surface salt accumulations in this coastal region resulted from a combination of the characteristic: **(i)** Mediterranean type climate, **(ii)** hydrogeology, **(iii)** saline seepages, and **(iv)** salt crusting formed on drain walls above sandy sulfuric and hypersulfidic materials. This chapter documents the first occurrence of sideronatrite [$Na_2Fe(SO_4)_2(OH).3H_2O$], tamarugite [$NaAl(SO_4)_2.6H_2O$] and alunogen in coastal acid sulfate soils in Australia, and these occur together with starkeyite ($MgSO_4.4H_2O$), pentahydrite ($MgSO_4.5H_2O$), blödite ($Na_2Mg(SO_4)_2.4H_2O$), gypsum and halite. The occurrence of these soluble salts represent changing surface flows (events) and ground water levels, which are linked to reclamation of the Gillman study area. Capillary action, combined with surface evaporation on the edge of the drains, has concentrated Fe-Al-Na-Mg sulfates, especially in summer or during dry periods. During drying events, soluble white sulfate-containing evaporite minerals, comprising starkeyite, pentahydrite and gypsum, precipitate as layers on the side of drains. Blödite forms on the surface of salt scalded areas containing sulfuric materials. Sideronatrite and tamarugite precipitated within yellowish-green, friable, 2 to 5 mm thick crusts on the sides of the drains. Sideronatrite (large platelets) is derived from the oxidation and dissolution of the sulfide framboids in saline sulfuric materials (< pH 2.5). Surrounding some of the crusts on the drain, where water temporarily leaches and ponds, sideronatrite dissolves and re-precipitates as schwertmannite within orange coloured patches. This process has been observed in inland acid sulfate soil systems (Fitzpatrick *et al.* 2010a; Thomas *et al.* 2009). These mineral precipitates play important roles in the transient storage of acidity and of components (Fe, Al, Na, Ca, Mg, Cl, Sr and SO_4), which may re-dissolve and contribute to the formation of pyrite and iron monosulfides in wetter soils such as stranded tidal creeks in the Gillman study site. The salts are likely to form as water levels decrease and have the potential to become a problem during seasonal re-flooding, if not managed properly, or through the re-establishment of tidal influences. Salt efflorescences containing blödite, tamarugite, pentahydrite, jarosite, gypsum and halite on salt flats or spoil piles (excavated) have potential for aerial entrainment and transport of trace elements and contaminants.

Although salt efflorescences have the ability to scavenge potentially toxic trace elements from soil pore waters and stream waters, thereby improving water quality, they are also a store of the sequestered trace elements and acidity which can be released. For

example, during rain events the salt efflorescences are dissolved and release stored contaminants and acidity to the drain or stream water as a pulse of higher concentration, which can be particularly deleterious to aquatic organisms (Brown *et al.* 1983; Romero *et al.* 2006).

Limiting the precipitation of salt efflorescences along drain walls would not reduce the total amount of trace elements potentially moving to drain waters, however it would allow for a more uniform flow of trace elements to the drain water rather than allowing large periodic fluxes of metals to enter the drain waters. This would be desirable for the preservation of downstream aquatic organisms. Limiting the accumulation of salt efflorescences may also reduce the risk of sulfide oxidation by ferric iron in downstream sediments, where water pH is slightly higher than in the drain near the source of the salts. These processes are collectively summarised in an evolutionary and predictive model (Figure 10-11). Limiting the precipitation and accumulation of salt efflorescences could be achieved by covering the drain walls to maintain humidity and slow evaporation at the soil surface (e.g. using mulching to cover drain walls or by installing pipes instead of using open drains). Ultimately, the best way to limit the problems associated with sulfuric, saline salt efflorescences would be to locate drains away from sulfuric and hypersulfidic materials. This could be done effectively with the aid of detailed soil maps of acid sulfate soil landscapes, such as those produced in Chapter 7 of this thesis.

The mineralogy, pH, Eh and geochemical composition of the soils and salt efflorescences may help explain the mobilisation of trace elements in acid sulfate soil environments. Scavenging of trace elements (As, Br, Ce, La, Mo and Sr) by sulfate salts was observed, but these elements were not detected in drain waters, even though most of the salts were dissolved during winter months. Gypsum, halite, jarosite, goethite and possibly hexahydrite did persist as solid phases during winter and may account for the sequestration of As, Mo, U and V by goethite, and Br, Ce, La and Sr by gypsum, halite and or hexahydrite. Scavenging of metals by carbonate minerals may have occurred in alkaline micro-environments. Seasonal formation of metal sulfides may also provide a sink for the trace elements, particularly Mo. Molybdenum appears to have accumulated in hypersulfidic soil materials near the base of the drain, which were subaqueous during winter months (Figure 10-11). Dilution may present an additional explanation for the

absence of trace elements in drain waters. This could be tested by achieving lower detection limits for analysis of water samples, as well as testing for a wider range of trace elements in the water samples.

Construction of open drains through map units 4, 5, 6 and 7 (Figure 7-2) should be avoided as similar conditions to those observed in the experimental drain are likely develop.

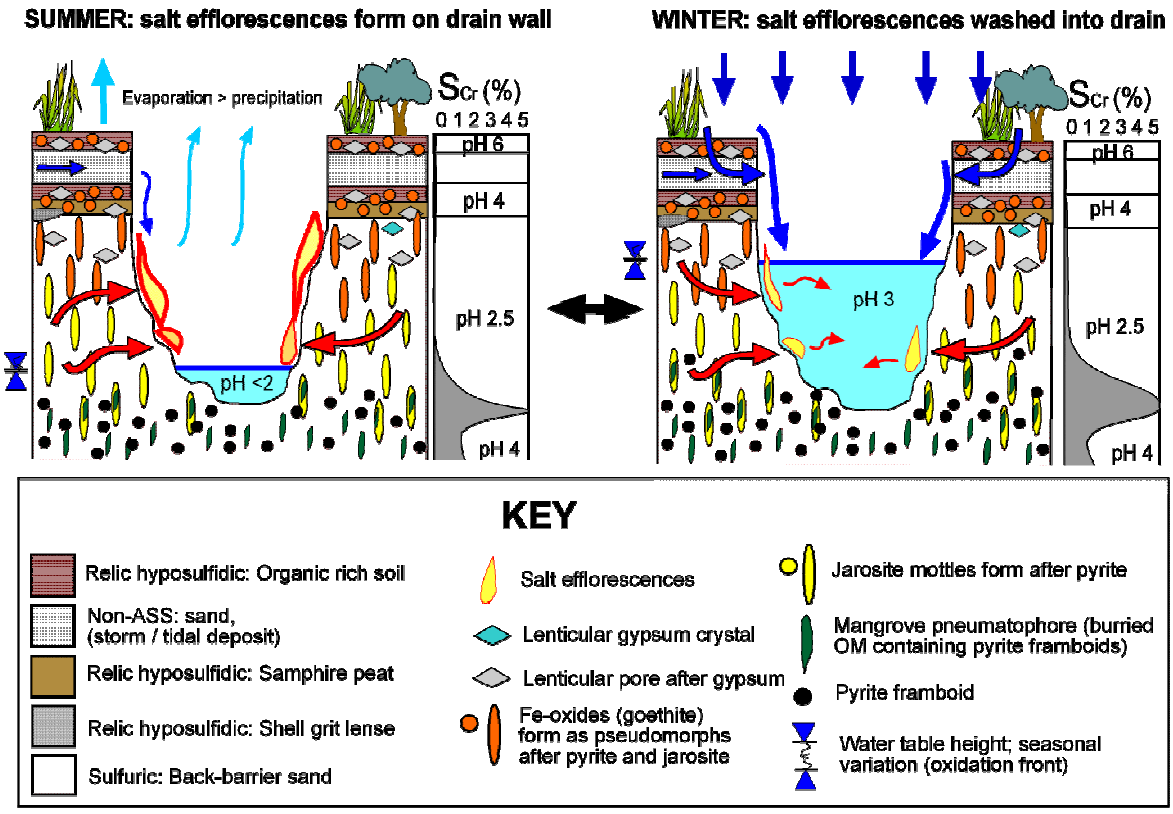

Figure 10-11 Predictive soil-regolith model (cross-section of the experimental drain) showing soil formation processes during: (i) summer (February 2003) with precipitation and accumulation of salt efflorescences on drain walls through element concentration at the surface by capillary action and evaporation and (ii) winter with dissolution of most salt efflorescences and subsequent flow into the drain water. Salt efflorescences are dominated by the widespread occurrences of goethite, jarosite, sideronatrite, tamarugite and metaalunogen together with other soluble minerals, including starkeyite, pentahydrite, gypsum and halite. Salt morphologies range from thin, powdery, very transient efflorescences to thicker, more persistent, soil-cementing crusts. The salt crusts form by the upward / sideways wicking of Na, Mg, Cl and SO_4 containing groundwaters and their subsequent concentration by surface evaporation. These Fe/Al oxyhydroxysulfate and oxyhydroxide minerals are indicators of very acidic soil conditions caused by pyrite oxidation and have the ability to accumulate trace elements by evaporative concentration of pore waters, or via erosion of surface soil layers. Rain events, during winter, cause water levels to rise and salts to dissolve, releasing acidity and trace elements to the drain water. The downward movement of sulfide oxidation products during summer may also contribute to the very high sulfide contents measured in organic rich soil layers near the base of the drain.